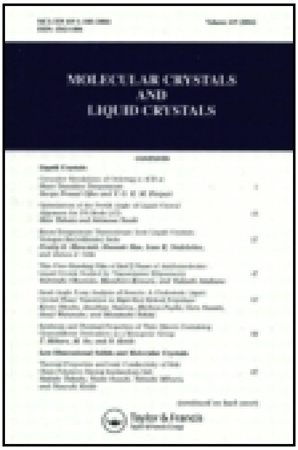

Molecular Crystals and Liquid Crystals

Publication details, including instructions for authors and subscription information:
http://www.tandfonline.com/loi/gmcl20

Dependence of Effective Doping Concentration on the Molecular Structure of Dopant: ABCV-P Doped OLEDs with Broad Range of and High Doping Concentration

Seung Han Lim [a], Gweon Young Ryu [b], Gu Young Kim [c], Ji Hoon Seo [c], Young Kwan Kim [c] & Dong Myung Shin [a]

[a] Department of Chemical Engineering, Hongik University, Seoul, Korea

[b] Department of Electric Information and Control Engineering, Hongik University, Seoul, Korea

[c] Center for Organic Materials & Information Devices (COMID), Hongik University, Korea

To cite this article: Seung Han Lim, Gweon Young Ryu, Gu Young Kim, Ji Hoon Seo, Young Kwan Kim & Dong Myung Shin (2008): Dependence of Effective Doping Concentration on the Molecular Structure of Dopant: ABCV-P Doped OLEDs with Broad Range of and High Doping Concentration, Molecular Crystals and Liquid Crystals, 491:1, 40-52

To link to this article: http://dx.doi.org/10.1080/15421400802328857

Mol. Cryst. Liq. Cryst., Vol. 491, pp. 40–52, 2008
Copyright © Taylor & Francis Group, LLC
ISSN: 1542-1406 print/1563-5287 online
DOI: 10.1080/15421400802328857

Dependence of Effective Doping Concentration on the Molecular Structure of Dopant: ABCV-P Doped OLEDs with Broad Range of and High Doping Concentration

Seung Han Lim[1], Gweon Young Ryu[2], Gu Young Kim[3], Ji Hoon Seo[3], Young Kwan Kim[3], and Dong Myung Shin[1]
[1]Department of Chemical Engineering, Hongik University, Seoul, Korea
[2]Department of Electric Information and Control Engineering, Hongik University, Seoul, Korea
[3]Center for Organic Materials & Information Devices (COMID), Hongik University, Korea

A new red fluorescent material, (2Z,2′Z)-3,3′-[4,4″-bis(dimethylamino)-1,1′:4′,1″-terphenyl-2′,5′-diyl]bis(2-phenylacrylonitrile) (ABCV-P), preventing concentration quenching in solid state was synthesized. Studies on the device performance of ABCV-P doped OLEDs with variation of the doping concentration and thickness of the emitting layer as well as the optical properties of ABCV-P were carried out. The effective doping concentration of ABCV-P dopant was in the range of 40%–50%. ABCV-P doped OLEDs showed maximum luminance of 11000 cd/m^2 (40%) and 6800 cd/m^2 (50%), CIE$_{xy}$ coordinates of (0.588, 0.410) (40%) and (0.597, 0.402) (50%) and full width at half maxima of 71 nm and 72.5 nm, respectively. Accordingly, ABCV-P doped OLED showed much lower sensitivity to doping concentration than the typical red doped ones.

Keywords: ABCV-P; concentration quenching; dopant molecular structure; effective doping concentration; red emissive; red doped OLEDs

1. INTRODUCTION

Organic light emitting diodes (OLEDs) have attracted broad interests due to their potential applications in full color flat panel displays. Efficient three primary colors, blue, green, and red are requisites for

---

This work was supported by the Brain Korea 21 Project & Seoul Research and Business Development Program (10555).

Address correspondence to Prof. Dong-Myung Shin, Department of Chemical Engineering, Hongik University Sangsu-Dong, Mapo-Gu, Seoul, 121-791, Korea. E-mail: shindm@wow.hongik.ac.kr

full color displays. Numerous fluorescent materials such as host-emitters or dopants have been known and developed since reports from Kodak on green OLED in 1987 and the green and red doped OLEDs in 1989 [1–2]. It has been reported some green and blue emissive materials used in OLEDs revealed high device performance but comparable red light emitting molecular materials are still rare in OLEDs application [3–4]. In the case of red fluorescent materials, they are highly susceptible to concentration quenching [4–5]. A universal method for solving the concentration quenching problem of red emissive materials caused when they are applied for OLEDs is the use of them as a dopant in the guest-host doped emitter system. In that system, concentration quenching can be avoided by dispersion and isolation of dopant molecules in the host materials. Red electroluminescence (EL) is usually achieved by doping red dyes into host materials with large band gap. In doped red OLEDs, the control of the dopant concentration is very critical because inefficient energy transfer from the host will result in a mixture of two emission profiles and contribute to an unsaturated red emission [6]. However, the optimum dopant concentration is usually low, commonly no greater than 2%, and the effective doping range is extremely narrow and commonly no greater than ±0.5% of the optimum concentration [4].

In this work, we report studies on the influence of dopant molecular structure on the effective doping concentration in red doped OLEDs as well as the optical and electroluminescent properties of a new red fluorescent material, (2*Z*,2′*Z*)-3,3′-[4,4″-bis(dimethylamino)-1,1′:4′,1″-terphenyl-2′,5′-diyl]bis(2-phenylacrylonitrile) (ABCV-P), which is designed and synthesized to prevent concentration quenching.

2. EXPERIMENTAL

2.1. Synthesis

Synthesis of ABCV-P was shown in Scheme 1. All solvents involved in the experiments were reagent grade and were purified by the usual methods before use. The molecular structure of ABCV-P was confirmed by ^{1}H and ^{13}C-NMR spectra of its precursors and MS (FAB) spectrum and elemental analysis (EA) of ABCV-P.

*2,5-Dibromoterephthalaldehyde (**I**).* was prepared by the method of the literature [7].

*4,4″-Bis(dimethylamino)-1,1′:4′,1″-terphenyl-2′,5′-dicarbaldehyde (**II**).* was obtained from the reaction of 2,5-dibromoterephthalaldehyde

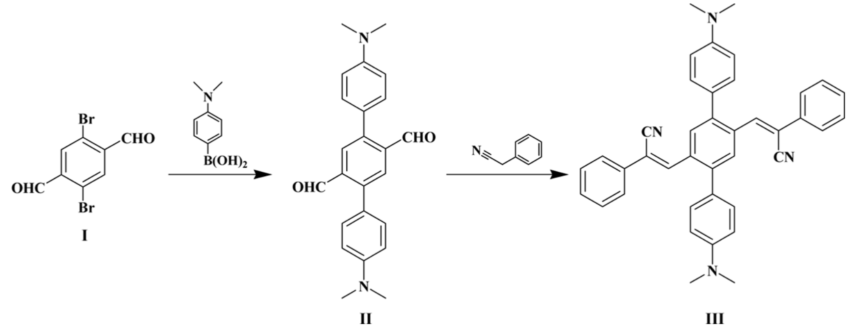

SCHEME 1 Synthesis of ABCV-P.

(I) with 4-(dimethylamino)phenylboronic acid by Suzuki coupling. The mixture of 2,5-dibromoterephthalaldehyde (I) (500 mg, 1.71 mmol), 4-(dimethylamino)phenylboronic acid (622 mg, 3.77 mmol), $Pd(PPh_3)_4$ (79 mg), Na_2CO_3 (540 mg) and Aliquat 336 (0.3 ml) in mixed solvent of toluene (40 ml)-H_2O (25 ml)-THF (10 ml) was mildly refluxed under N_2 atmosphere with stirring for 3 hr. The reaction mixture was cooled, filtered and washed with water and n-hexane. Removal of the solvents and drying under high vacuum afforded 600 mg (1.61 mmole) of the product (II) as a light yellow to orange solid and further purification was not required. Yield: 94%; ^{1}H-NMR (500 MHz, $CDCl_3$) δ (ppm) 10.105 (s, 2H), 8.060 (s, 2H), 7.315 (d, 4H), 6.830 (d, 4H), 3.048 (s, 12H); ^{13}C-NMR (125 MHz, $CDCl_3$) δ (ppm) 192.85, 192.80, 150.45, 143.64, 136.36, 131.07, 129.88, 123.00, 112.15, 40.33.

(2Z,2′Z)-3,3′-[4,4″-bis(dimethylamino)-1,1′:4′,1″-terphenyl-2′,5′-diyl]-bis(2-phenylacrylonitrile) (III), ABCV-P. was prepared from the Knoevenagel reaction of 4,4″-bis(dimethylamino)-1,1′:4′,1″-terphenyl-2′,5′-dicarbaldehyde (II) with benzyl cyanide. The mixture of 4,4″-bis(dimethylamino)-1,1′:4′,1″-terphenyl-2′,5′-dicarbaldehyde (II) (800 mg, 2.15 mmol), benzyl cyanide (630 mg, 5.38 mmol) and sodium ethoxide (prepared by reaction of 123 mg of Na with 10 ml of absolute EtOH) in 210 ml of EtOH was stirred at room temperature for 4 day. The red solid formed in reaction mixture was filtered and washed with water, EtOH and n-hexane. The filtrate was further purified by recrystallization in $CHCl_3$/Acetone. Removal of the solvents and drying under high vacuum afforded 717 mg (1.26 mmole) of the product (III) as a red solid. mp 324°C; Yield: 58.6%; MS (FAB) calcd for $C_{40}H_{34}N_4$ (M^+) m/z 570, found 570; Anal. calcd. for $C_{40}H_{34}N_4$: C: 84.19, H: 5.74, N: 9.79. Found: C: 84.18, H: 6.00, N: 9.82.

2.2. Measurement

^{1}H-NMR and ^{13}C-NMR spectra were recorded on a Varian Unity INOVA 500 spectrometer operating at 499.761 MHz and 125.701 MHz, respectively. Mass spectrum (FAB-MS) was measured on JEOL, JMS-AX505WA, HP 5890 Series II Hewlett-Packard 5890 A (capillary column) using standard conditions. Elemental analysis was performed on a CE instrument EA 1110 analyzer. The melting point was measured to be 324°C by differential scanning calorimetry (DSC) using a Seiko Exstar 6000(DSC6100) with a scan rate of 10°C/min at the temperature of 40°C ~ 400°C. UV-visible absorption and PL spectra were measured by HP model 8453 and Perkin Elmer LS-50B, respectively.

The AFM measurement was performed using NS4A in the tapping mode, on a 1 μm × 1 μm scale. The HOMO and LUMO energy levels of ABCV-P were obtained from cyclic voltammetric method using a Kosentech KST-P1 at a scan rate of 50 mV/s with ABCV-P thin film deposited on indium tin oxide (ITO) substrate as the sample, dimethylformamide (DMF) as the solvent and tetrabutylammonium tetrafluoroborate (n-Bu_4NBF_4) as the electrolyte (0.05 M). Electroluminescence spectra and brightness-current-voltage characteristics of the device were measured using keithley 238, CHROMA METER CS-100A and LS 50B. All the measurement was carried out at room temperature.

2.3. Fabrication of OLED

The OLED was fabricated by the high vacuum thermal deposition (8×10^{-1} torr) of organic materials onto the surface of ITO coated glass substrate. An ITO coated glass was cleaned in an ultrasonic bath by regular sequences: in acetone, methanol, diluted water and isopropyl alcohol. The cleaned substrate was immediately loaded into the deposition chamber in order to prevent air contamination. The structure of fabricated device was ITO/NPB (50 nm)/MADN:ABCV-P (x%) (30 nm)/BCP (10 nm)/Alq_3 (20 nm)/Liq (2 nm)/Al (100 nm), in which NPB, ABCV-P, BCP, Alq_3 and Liq were used as a hole transporting layer (HTL), an emitting layer (EML), a hole blocking layer (HBL), an electron transporting layer (ETL) and an electron injection layer (EIL), respectively.

3. RESULTS AND DISCUSSION

One type of red emissive material that may be most commonly used in OLEDs has electron donor and acceptor (D-A) groups on opposite sides of the molecule with strong charge transfer (CT) [4]. This red fluorescent material is vulnerable to concentration quenching in solid state owing to dipole-dipole interactions among the molecules. The charge-transporting property and the luminescent performance of emitter depend on the structure of the molecule such as the conjugated structure of the molecule [5], molecular planarity and rigidity. Figure 1 (a) shows the characteristic molecular structure of a new red fluorophore, ABCV-P, which is prevented from concentration quenching in solid state. This molecule has a strong intramolecular charge transfer (ICT) character with two identical pairs of electron donor and acceptor (D-A) groups. In spite of having ICT, the new red emissive material, ABCV-P, can be prevented from concentration quenching because dipole-dipole interactions among the molecules are almost suppressed by reducing the net molecular dipolemoment due to the cross

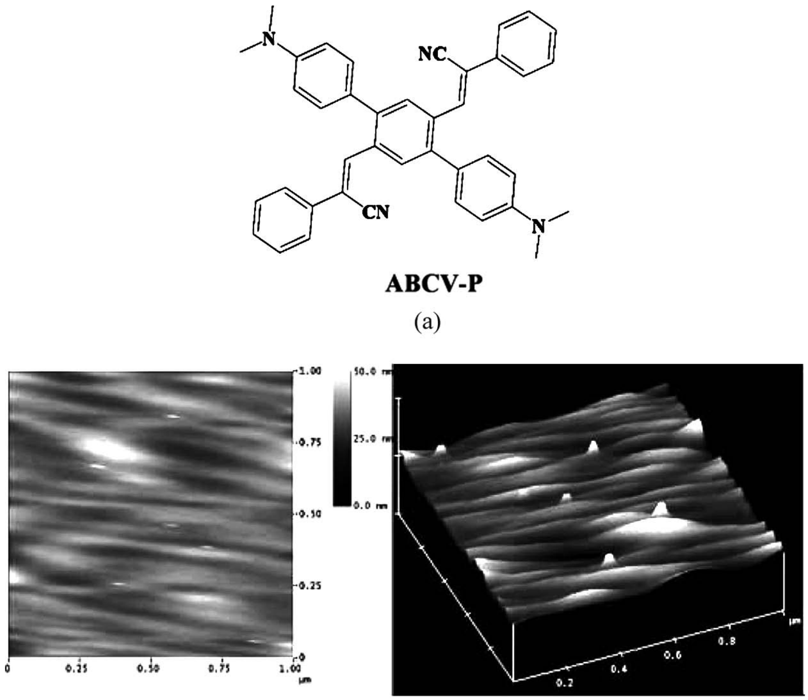

(a)

(b)

FIGURE 1 The molecular structure of ABCV-P (a) and the AFM topographic image (1 μm × 1 μm), measured by tapping-mode, of ABCV-P thin solid film in ITO/NPB (40 nm)/ABCV-P (80 nm), in which roughness (R_{rms}) value of ABCV-P thin film was measured to be 2.7 nm.

arrangements of donor-donor and acceptor-acceptor pairs. Moreover, because of twisted terphenyl backbone structure and seriously distorted molecular geometry around central benzene ring caused by steric crowding of substituents on that, the molecular structure of this red emissive material is noncoplanar so that the unfavorable intermolecular interactions affecting photoluminescence and electroluminescence occurring in solid state can be reduced very well. This was well supported by the analysis based on atomic force microscopy (AFM). Figure 1 (b) shows the result of AFM measurement ($R_{rms} = 2.67\,nm$) on ABCV-P thin film, in which ABCV-P thin film exhibits soft surface state without crystalline packing. An amorphous or badly crystal film is favorable in OLEDs [8–10].

Figure 2 (a) shows UV-visible absorption and PL spectrum of ABCV-P and PL spectrum of host material, MADN and Figure 2 (b) does the schematic energy band diagram of the device with the structure of ITO/NPB/MADN:ABCV-P/BCP/Alq_3/Liq/Al where the energy levels of MADN and ABCV-P were obtained by the cyclic voltammetric method. The UV-visible absorption and photoluminescence (PL) spectra were measured in chloroform solution. The absorption and emission of ABCV-P was peaked at 334 nm with shoulder at 440 nm and 588 nm, respectively. The PL emission of ABCV-P showed large Stokes shift. Owing to the large Stokes shift, there was hardly an overlap between absorption and emission of light by the ABCV-P molecule. This leads to little self-absorption of the emitted light so that the ABCV-P is very advantageous for OLED application [5].

The effects of doping concentrations (x) on the performance of ABCV-P doped OLEDs are well shown in Figure 3. Figure 3 (a) shows the normalized EL spectra of the ABCV-P doped OLEDs at 6 V and different doping concentrations ($x = 10\%$, 20%, 35%, 40% and 50%), respectively. Emissions at low doping concentrations ($x = 10\%$, 20% and 30%) showed stronger luminescence in orange and orange-red regions, which resulted out bad chromaticity, than those at high doping concentration ($x = 40\%$ and 50%). The chromaticity of ABCV-P doped OLED was improved to red ($CIE_{xy} = 0.597$, 0.402) by increasing the dopant concentration to 50% but there was not a further improvement by increasing that. Figure 3 (b) and (c) show the current density *vs.* voltage (I-V) and current density *vs.* luminance (I-L) and luminous efficiency (inset) (I-LE) of the ABCV-P doped OLEDs at various doping concentrations of 10%, 20%, 30%, 40% and 50%, in which the luminance maxima are 22200 cd/m^2 (at 565 mA/cm^2), 18000 cd/m^2 (at 578 mA/cm^2), 12600 cd/m^2 (at 630 mA/cm^2), 11000 cd/m^2 (at 690 mA/cm^2) and 6800 cd/m^2 (at 712 mA/cm^2), respectively. Selected EL performance of the ABCV-P doped OLEDs with the MADN host

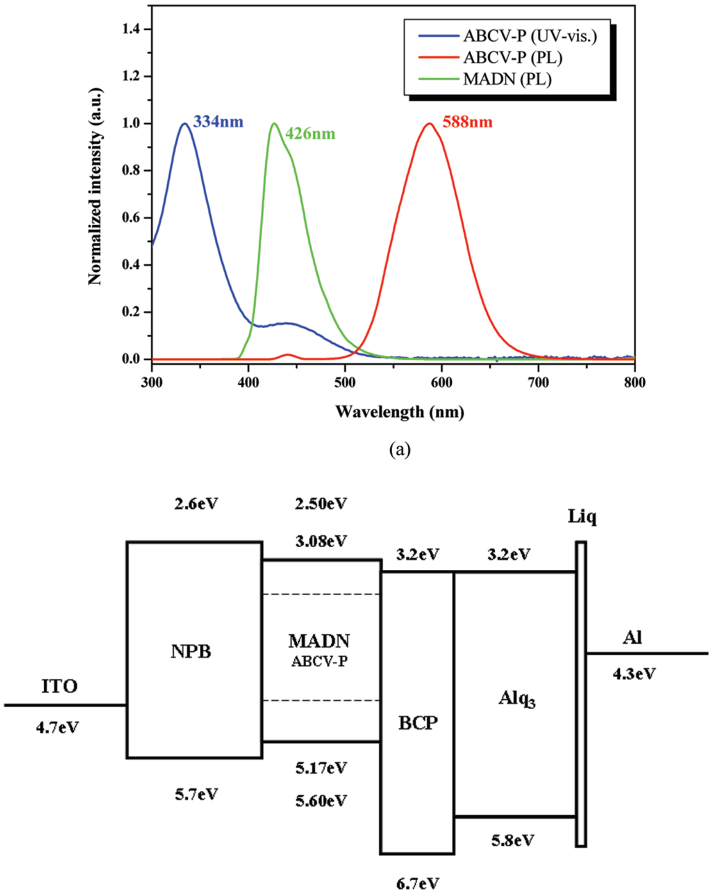

(a)

(b)

FIGURE 2 UV-visible absorption and PL spectra of ABCV-P and PL spectrum of host material, MADN in chloroform (a) and the schematic energy band diagram of the device, ITO/NPB/MADN: ABCV-P/BCP/Alq_3/Liq/Al (b).

material at various doping concentrations was summarized in Table 1. As shown in Figure 3 (a), EL emission of ABCV-P doped device at doping concentration of 50% showed the best red color. EL emission of that at doping concentration of 40% showed slightly blue shift and stronger electroluminescence in orange-red region compared to that of 50%. To investigate the effect of thickness of emitting layer, study on device at doping concentration of 40% with varying the thickness of that ($y = 10$ nm, 20 nm, 30 nm and 40 nm) was carried out. Figure 4

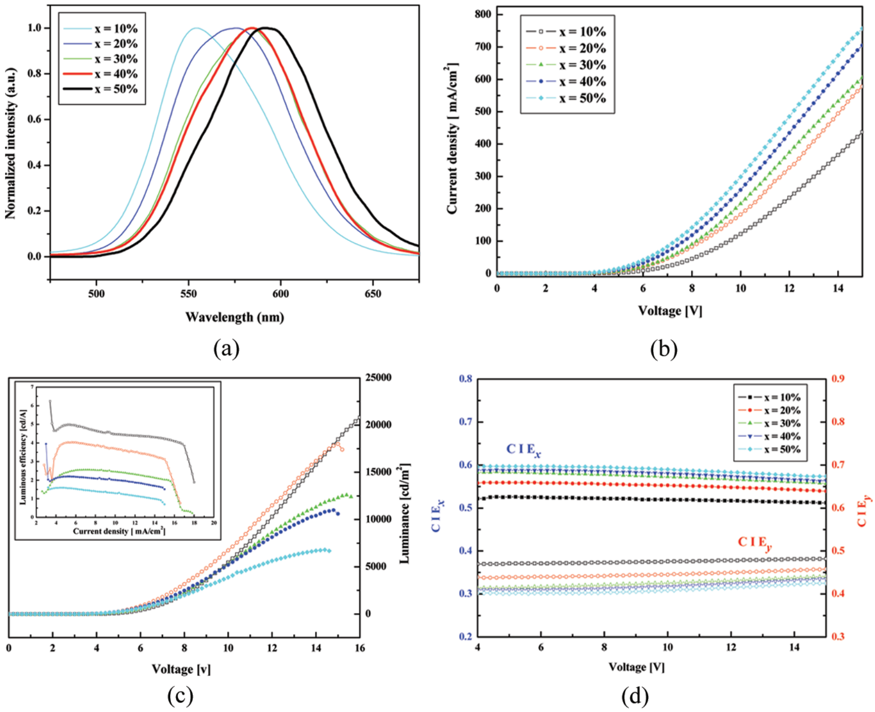

FIGURE 3 The effect of dopant concentration (x) on the performance of ABCV-P doped device, ITO/NPB (50 nm)/MADN:ABCV-P (x%) (30 nm)/BCP (10 nm)/ Alq_3(20 nm)/Liq (2 nm)/Al (100 nm): normalized EL spectra of the ABCV-P doped OLEDs at 6 V (a), the current density *vs*. voltage (I-V) characteristics (b), current density *vs*. luminance (I-L) and luminous efficiency (inset) (I-LE) (c) and CIE_{xy} coordinates with varying the voltage at different doping concentration (x = 10%, 20%, 35%, 40% and 50%), respectively.

shows the effect of thickness (y) of emitting layer on the performance of ABCV-P doped OLEDs at doping concentration of 40% and the results were summarized in Table 2. EL emission peaks of the devices with thickness of 20 nm and 40 nm were measured to be the best (λ_{max}^{EL} = 588.5 nm). However, based on device performance including full width at half maximum (FWHM), luminance (cd/m^2), luminous efficiency (cd/A) and color chromaticity (CIE_{xy} coordinates), the performance of device with emitting layer thickness of 40 nm is better than that of 20 nm. At effective doping concentration (40% and 50%), CIE_{xy} coordinate of (0.60, 0.40) for ABCV-P doped OLED is medium range compared to those for traditional red, such as DCM

TABLE 1 Performance of ABCV-P doped devices with variation of the doping concentration

(%)	Max. current density (mA/cm^2)	Luminance (cd/m^2) max, @ 100mA/cm^2, @ 20mA/cm^2	Max. luminous efficiency (cd/A)	$\lambda_{max}{}^{EL}$ (nm)	FWHM (nm)	CIE (x, y)
10	631, 18 V	22200, 4540, 971	4.98, 5.2 mA/cm^2	554.5	68.5	0.525, 0.471
20	661, 16 V	18000, 3880, 803	4.03, 5.2 mA/cm^2	576	75.5	0.555, 0.443
30	667, 16 V	12600, 2550, 508	2.56, 5.2 mA/cm^2	583	73.5	0.581, 0.417
40	705, 15 V	11000, 2100, 444	2.20, 5.2 mA/cm^2	584.5	71	0.588, 0.410
50	757, 15 V	6800, 1460, 312	1.59, 5.2 mA/cm^2	591	72.5	0.597, 0.402

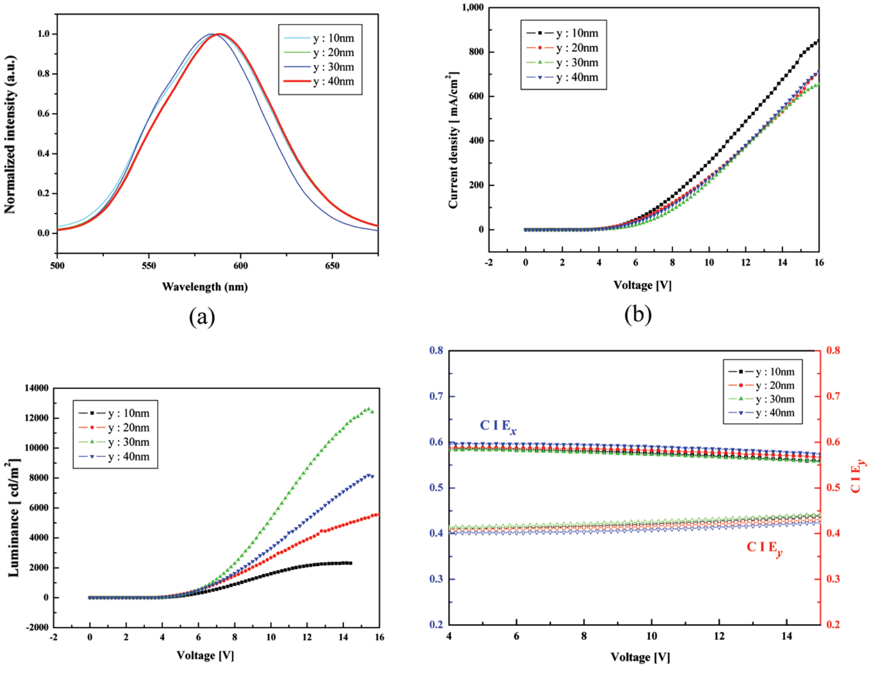

(a) (b) (c) (d)

FIGURE 4 The effect of thickness (y) of emitting layer on the performance of ABCV-P doped OLEDs at doping concentration of 40%, ITO/NPB (50 nm)/MADN:ABCV-P (40%) (y nm)/BCP (10 nm)/Alq_3(20 nm)/Liq (2 nm)/Al(100 nm):normalized EL spectra of the ABCV-P doped OLEDs at 6 V (a), the current density *vs.* voltage (I-V) characteristics (b), current density *vs.* luminance (I-L) (c) and CIE_{xy} coordinates with varying the voltage at various thickness of emitting layer (y 10 nm, 20 nm, 30 nm and 40 nm), respectively.

derivatives ($x = 0.58 \sim 0.64$, $y = 0.41 \sim 0.36$) [4,11] and DCJTB derivatives ($x = 0.60 \sim 0.65$, $y = 0.35 \sim 0.33$) [4,12], doped OLEDs. Furthermore, ABCV-P doped OLEDs showed narrow FWHM (68.5 ~ 74.5 nm) compared to those of DCM derivatives-doped OLEDs (FWHM = 81 ~ 92 nm) [13]. Therefore, although further investigation is still required, effective range of doping concentration for ABCV-P must be much broader compared to those for typical red dopants. As previously mentioned, the optimum dopant concentration of typical red emitting materials is commonly no greater than 2% and their effective doping range is extremely narrow and commonly no greater than ±0.5% of the optimum concentration. The EL characteristics using ABCV-P

TABLE 2 Performance of ABCV-P doped devices at various thickness of emitting layer

	Max. current density (mA/cm^2)	luminance (cd/m^2) max, @ 100 mA/cm^2, @ 20 mA/cm^2	Max. luminous efficiency (cd/A)	$\lambda_{max}{}^{EL}$ (nm)	FWHM (nm)	CIE (x, y)
10 nm	876, 16.6 V	2320, 621, 138	0.71, 4.2 mA/cm^2	586.5	77	0.582, 0.415
20 nm	713, 16 V	5560, 1225, 267	1.37, 4.2 mA/cm^2	588.5	75	0.587, 0.411
30 nm	705, 15 V	11000, 2113, 438	2.2, 5.2 mA/cm^2	584.5	71	0.588, 0.410
40 nm	713, 16 V	8200, 1475, 297	1.49, 5.4 mA/cm^2	588.5	74.5	0.596, 0.402

TABLE 3 Comparison of EL characteristics of ABCV-P and typical red dopants at effective doping concentration

Red doping	Dopant concentration (%)	Luminance (cd/m^2) max at $100\,mA/cm^2$, at $20\,mA/cm^2$	λ max^{EL} (nm)	CIE (x, y)
ABCV-P[a]	30	12600, 2550, 508	583	0.581, 0.417
	40	11000, 2100, 444	584.5	0.588, 0.410
	50	6800, 1460, 312	591	0.597, 0.402
DCM2[b]	2	7780, –, –	644	0.640, 0.360
DCM2[c]	10	1400, –, –	650	0.640, 0.360
DCJTB[d]	1	15000, 6000, 1200	628	0.620, 0.380

[a] ITO/NPB/MADN:ABCV-P(x%)/BCP/Alq_3/Liq/Al.

[b] ITO/CuPc/NPB/Alq_3: rubrene(5%):DCM2(2%)/Mg:In.

[c] ITO/NPB/Alq_3:DCM2(10%)/Mg:Ag.

[d] ITO/NPB/Alq_3:QAD(0.5%):DCJTB(1%)/Alq_3/LiF/Al.

and some typical red fluorescent materials as dopants were summarized in Table 3 [4].

4. CONCLUSIONS

A new red emissive material, ABCV-P, designed to be prevented from fluorescence concentration quenching in solid state was synthesized to decrease sensitivity to doping concentration, which was drawbacks in typical red, such as DCM-type dye, doped OLEDs, by increasing the effective doping concentration. ABCV-P doped OLEDs exhibited medium to high device performance compared to those of typical red doped ones. Furthermore, the effective doping concentration of ABCV-P doped device was dramatically increased to much higher than those of traditional red, such as the DCM derivatives, doped OLEDs and the sensitivity to doping concentration was decreased much lower than that of typical red doped device. Therefore, we concluded that the effective doping concentration of red doped OLEDs could be controlled by design of dopant molecular structure to suppress concentration quenching and this was very crucial for mass production of OLEDs.

REFERENCES

[1] Tang, C. W. & VanSlyke, S. A. (1987). *Appl. Phys. Lett.*, *51*, 913.
[2] Tang, C. W., VanSlyke, S. A., & Chen, C. H. (1989). *Appl. Phys.*, *65*, 3610.
[3] Fu, H., Zhan, Y., Xu, J., Hou, X., & Xiao, F. (2006). *Optical Materials.*, *29*, 348.

[4] Chen, C. -T. (2004). *Chem. Mater.*, *16*, 4389.

[5] Burrows, P. E., Forrest, S. R., Sibley, S. P., & Thompson, M. E. (1996). *Appl. Phys. Lett.*, *69*, 2959.b.

[6] Hamada,Y., Kanno, H., Tsujioka, T., & Takahashi, H. (1999). *Appl. Phys. Lett.*, *75*, 1682.

[7] Evers, Robert C., & Moore, George J. (1988). "Ethynyl-containing aromatic polyamide resin," U.S. Patent, 4,752,642

[8] Liu, Z., Chen, Z. -J., & Gong, Q.-H. (2005). *Chin. Phys. Lett.*, *22*, 1536.

[9] Wu, W. -C., Yeh, H. -C., Chan, L. -H., & Chen, C. -T. (2002). *Adv. Mater.*, *14*, 1072

[10] Thomas, K. R. J., Lin, J. T., Tao, Y. -T., & Chuen, C. -H. (2002). *Adv. Mater.*, *14*, 822.

[11] Xiao, J., Yao, Y., Deng, Z., Wang, X., & Liang, C.-J. (2007). *Journal of Luminescence.*, *639*, 122–123.

[12] Li, F., Lin, J., Feng, J., Cheng, G., Liu, H., Zhang, S. L. L., Zhang, X., & Lee, S.T. (2003). *Synthetic Metals*, *139*, 341–346.

[13] Yang, L., Guan, M., Nie, D., Lou, B., Liu, Z., Bian, Z., Bian, J., & Huang, C. (2007). *Optical Materials*, *29*, 1672–1679.